Determination of slip modulus of cold-formed steel composite members sheathed with plywood structural panels

Dheeraj Karki[1], Harry Far[*1], Suleiman Al-hunity[1]

[1] *School of Civil and Environmental Engineering, Faculty of Engineering and Information Technology, University of Technology Sydney (UTS), Building 11, Level 11, Broadway, Ultimo, NSW 2007, Australia*

Abstract. An experimental investigation to study the behaviour of connections between cold-formed steel (CFS) joist and plywood structural panel is presented in this paper. Material testing on CFS and plywood was carried out to assess their mechanical properties and behaviour. Push-out tests were conducted to determine the slip modulus and failure modes of three different shear connection types. The employed shear connectors in the study were; size 14 (6mm diameter) self-drilling screw, M12 coach screw, and M12 nut and bolt. The effective bending stiffness of composite cold-formed steel and plywood T-beam assembly is calculated based on the slip modulus values computed from push-out tests. The effective bending stiffness was increased by 25.5%, 18% and 30.2% for self-drilling screw, coach screw, nut and bolt, respectively, over the stiffness of cold-formed steel joist alone. This finding suggests the potential to enhance the structural performance of composite cold-formed steel and timber flooring system by mobilisation of composite action present between timber sheathing and CFS joist.

Keywords: Cold-Formed Steel Joists; Structural plywood; Material tests; Push-out tests; Load-slip behaviour; Slip modulus

1. Introduction

Cold-formed steel members are becoming a popular material for both commercial and residential construction around the world which can be used in the construction of roofs, walls and floors (Saleh et al., 2018). The popularity of the cold-formed steel members is because of the high strength to weight ratio, ease of fabrication and rapid construction (Wang and Young, 2014; Kyvelou et al., 2018). Cold-formed steel beams sheathed with timber floorboards attract the building professionals' interest to construct a lightweight flooring system (Karki and Far, 2021; Zhou et al., 2019). A few studies (Xu and Tangorra, 2007; Parnell et al., 2010) in composite cold-formed steel and timber flooring system, primarily to investigate the dynamic behaviour were carried out in the past. Due to the lack of proper design guidelines, the beneficial shear interaction between timber sheathing and CFS joists is often ignored, which leads to conservative designs. For the first time, studies (Kyvelou et al., 2017, 2018; Zhou et al., 2019) on composite cold-formed steel and timber flooring system were conducted on the flexural capacity of the flooring system, taking into account the effect of composite action.

Composite action is a widely known mechanism used throughout engineering in composite structures (Tabatabaiefar et al., 2017; Far, 2019). The main advantage of composite structure over non-composite structure is that they generally provide overall more significant performance than the sum of their individual parts, which means an increase in structural capacity and contribute to the minimal utilisation of resources by reducing the size of structural members (Loss and Davison, 2017; Hassanieh et al., 2016). For the two members of a composite assembly to act as one, a means to transfer the developed shear forces must be present. The shear transfer can be achieved through different methods, but the most common in cold-formed steel composite structures are mechanical fasteners and interlocking members (Lakkavalli and Liu, 2006). It is well understood that the degree of shear connection and its ductility have a significant influence on the structural performance of the composite system, but it is until recently researchers have started to investigate on the field of composite cold-formed steel and timber flooring systems. Experimental and numerical investigations carried out by (Kyvelou et al., 2017, 2018) have shown a 140% increase in bending capacity and a 40% increase in flexural stiffness by utilising the benefits of composite action. Li et al. (2012), Far (2020), and Karki et al. (2021) has highlighted the importance of shear connection and its influence on the bending strength and stiffness of the composite cold-formed steel and timber flooring system.

Self-drilling screws were used to connect the timber floorboard with the cold-formed steel in the previous research studies, which is common in the construction industry. However, there is a need to investigate different types of shear connectors to better understand the composite behaviour in this type of construction. Hence, the focus of this study is to understand the load-slip behaviour of three different types of connections: self-drilling screw, coach screw, and nut and bolt. In this study, the performance of the

[*]Corresponding author, PhD. Senior lecturer in Structural Engineering

Email: Harry.Far@uts.edu.au

CFS-plywood composite connection in terms of slip modulus and ductility is experimentally investigated. The short-term load-slip response, ultimate load carrying capacity, and failure mode of CFS-plywood composite connections were studied by conducting push-out tests. The slip modulus values determined from the push-out tests have been used to compute the effective bending stiffness of the composite assembly.

2. Experimental Program

Material tests were conducted to determine the material characteristics of the structural components used in the composite system, and push-out tests were conducted to determine the load-slip response of the shear connectors. Fig.1 shows the cross-sectional dimensions of the CFS C-section joist utilised in the push-out tests. 45mm thick structural plywood panels (F11 structural grade) shown in Fig. 2, made out of radiate pine was used as timber sheathing. A comprehensive testing program in accordance with the relevant Australian Standards was carried out to obtain the mechanical properties of the materials used in the push-out tests.

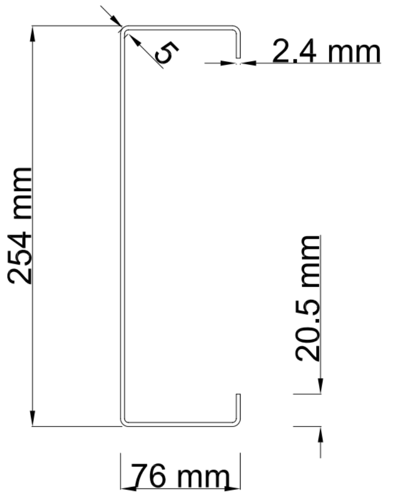

Fig.1 Cross-section dimensions of CFS joist

Fig. 2 Tested plywood material

2.1 Material Tests

2.1.1 Cold-formed steel tensile tests

Tensile steel coupon tests were conducted to determine the mechanical properties of the cold-formed steel joists. All the cold-formed steel sections used in this study were supplied by Fielders Pty Ltd. The dimensions of the tensile coupon are illustrated in Fig.3(a). The coupons were extracted from the web and flange of the different CFS joists. Eight tests were carried out. Tensile coupon specimen before and after the test is shown in Fig.3(b) and 3(c).

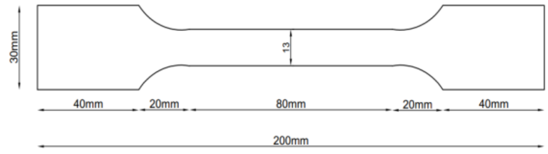

Fig. 3(a) Dimension of the tensile coupon

Fig. 3(b) Tensile coupon with strain gauge attached

Fig. 3(c) Failure of CFS coupon during tensile testing

The coupon preparation and tests were carried out following AS1391:2007 (Standard Australia, 2007). Two strain gauges were attached to each side of the coupons to measure strain accurately. The tests were conducted using a 100 kN Shimadzu tensile testing machine (AGX-100 kN) under displacement control. The results obtained from the tensile coupon tests are presented in Table 1, and the stress-strain curves are shown in Fig. 4.

Table 1 Mechanical properties obtained from the tensile coupon test

Specimens	Elastic modulus E (GPa)	Yield strength $\sigma_{0.2}$ (MPa)	Tensile strength σ_u (MPa)	Elongation at fracture ε_f (%)
SP-1	206	502	556	14
SP-2	202	509	560	18
SP-3	210	496	612	11
SP-4	205	512	564	9
SP-5	207	502	547	15
SP-6	208	507	572	14
SP-7	206	504	556	12
SP-8	210	501	564	12
Average	207	504	566	

Minimum yield strength according to the manufacturer is 450 MPa.

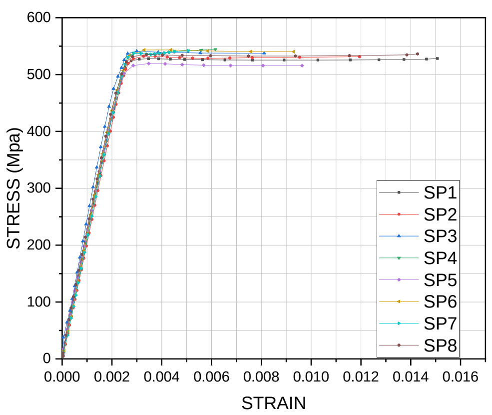

Fig. 4 Stress-strain curve obtained from tensile coupon tests

2.1.2 Plywood tests

Test samples obtained from 45 mm thick structural plywood panels were tested to determine its bending strength, compression strength, tensile strength and modulus of elasticity. All the plywood panels used in this study were made from Radiata Pine and were supplied by Big River Group Pty Ltd. The test specimen preparation and testing procedure were conducted in accordance with AS/NZS 2269-1:2012 (Standard Australia, 2012). Four repeated tests were conducted for each test type.

Bending, compression and tensile test

Test pieces were cut from the plywood panels as shown in Fig. 5 in accordance with AS/NZS 2269.1. The cutting pattern allows for both the parallel (pa) and perpendicular (pe) specimens from the plywood panels of standard dimensions (2400 mm x 1200 mm). The test pieces for bending (shown as B_{pa} or B_{pe}) and compression (C_{pa} or C_{pe}) were 300 mm wide, and the tension (T_{pa} or T_{pe}) test pieces were 150 mm wide.

Four-point bending tests were conducted on the specimens cut from the plywood panels. The strength and stiffness properties of the plywood were determined for the panels cut in both parallel and perpendicular directions. The typical arrangement of the four-point bending test is shown in Fig. 6. The load was applied through a 300 kN hydraulic actuator at a constant rate of 4mm/min until failure. Two lasers were used to measure the vertical deflections at mid-span. All the specimen failures occurred within 3-5 minutes as specified in the standard. Fig. 7 illustrates a typical bending failure at about the mid-span of the specimen.

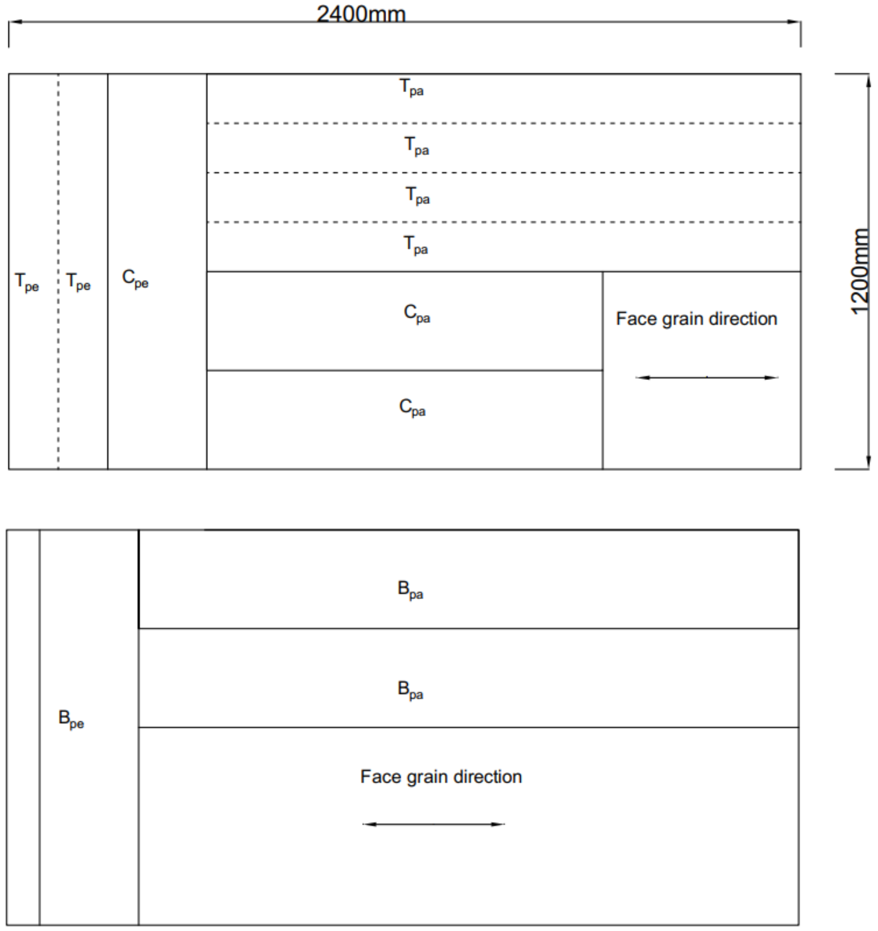

Fig. 5 Cutting pattern for the structural plywood test panel

The measured strength and modulus of elasticity in bending of the parallel and perpendicular cut specimens are presented in Table 2. In addition to the bending test, tensile and compressive tests on the parallel and perpendicular cut specimens were carried out per AS/NZS 2269-1:2012. As specified in the standard, the rate of load application was adjusted so that the failure of the test pieces occurred within the 4-5 minute range. The calculated compression and tensile strength are presented in Table 2. Parallel test pieces are labelled as 'Par'-followed by the specimen number, while perpendicular test pieces are labelled as 'Per'-followed by the specimen number.

2.2 Push-out Tests

2.2.1 Push-out specimens

Laboratory push-out tests on three major groups of CFS-plywood connections have been performed, and each group consist of three identical specimens. A total of nine push-out specimens were fabricated and tested. The details of the push-out specimens are given in Table 3. In Table 3, specimens are labelled by the letter 'P', indicating a push-out specimen, followed by connection types. For e.g., 'P-SDS' is the push-out test series that utilises self-drilling as shear connectors. The geometry and set-up adopted for the tests are shown in Fig. 8. The primary variables considered in the experimental program were three different types of connections; self-drilling screws, coach screws, nut and bolt. As shown in Fig. 8, two rows of fasteners at 200 mm spacing are used for the tests.

Self-drilling screws (14 gauge), coach screws (Size M12), nut and bolt (Size M12) were used in the testing as a means of shear connections. The basic mechanical properties of the shear connectors are given in Table 4. Coach screw, and nut and bolt were made of Grade 4.6 steel with nominal yield and ultimate strength of 240 MPa and 400 MPa. Self-drilling screws, coach screws and bolts comply with the requirements of AS 3566.1 (Standard Australia, 2002) , AS 1393 (Standard Australia, 1996) , AS 1110.1 (Standard Australia, 2000) respectively. The outline of fasteners used in the push-out tests is shown in Fig. 9.

Table 2 Measured strength and stiffness properties of tested plywood specimen

Specimen	Bending strength (MPa)	Compression strength (MPa)	Tension strength (MPa)	Modulus of Elasticity in bending (MPa)
Par-1	42.5	32	24.2	9877
Par-2	46	30.7	20.6	9780
Par-3	36	32	25	8497
Par-4	35.75	31.15	22.8	9006
Perp-1	46	29	16.2	9730
Perp-2	49.8	26.4	14	7738
Perp-3	50.15	29.1	17	8927
Perp-4	36	28	16.8	6796

Fig. 6 Four-point bending test arrangement

Fig. 7 Typical bending failure on tensile face of plywood panel

Table 3 Summary of push-out specimen details

Test series	Type of connection	Number of specimens tested
P-SDS	Self-drilling screw (6mm diameter)	3
P-CS	Coach screw (M12)	3
P-NB	Nut and bolt (M12)	3

2.2.2 Experimental setup, fabrication and instrumentation

The push-out tests configuration can influence the test results due to the unnecessary friction between different components of the specimen and asymmetrical load distribution on the specimen (Hassanieh et al., 2017). Hence, two CFS joists joined back to back, and two plywood panels were mechanically connected on both flange sides, as shown in Fig. 8 arrangement was adopted in this study to ensure a stable setup.

After cutting the plywood panels to the required size, both the plywood panels and the flange of the CFS C-section were predrilled except for the specimen with the self-drilling screw. The diameter of the predrilled holes in the plywood panels was 1 to 1.5 mm smaller than the diameter of the coach screws and 0.5 to 1.5 mm larger than the diameter of the bolts. The diameter of the predrilled holes in the flange of the C-section was 0.2 to 0.6 mm larger than the connectors (screws and bolts).

The overall experimental setup is shown in Fig. 10. A 300 kN load-cell was used for the testing of push-out specimens. The relative displacement or slip between the CFS beam and

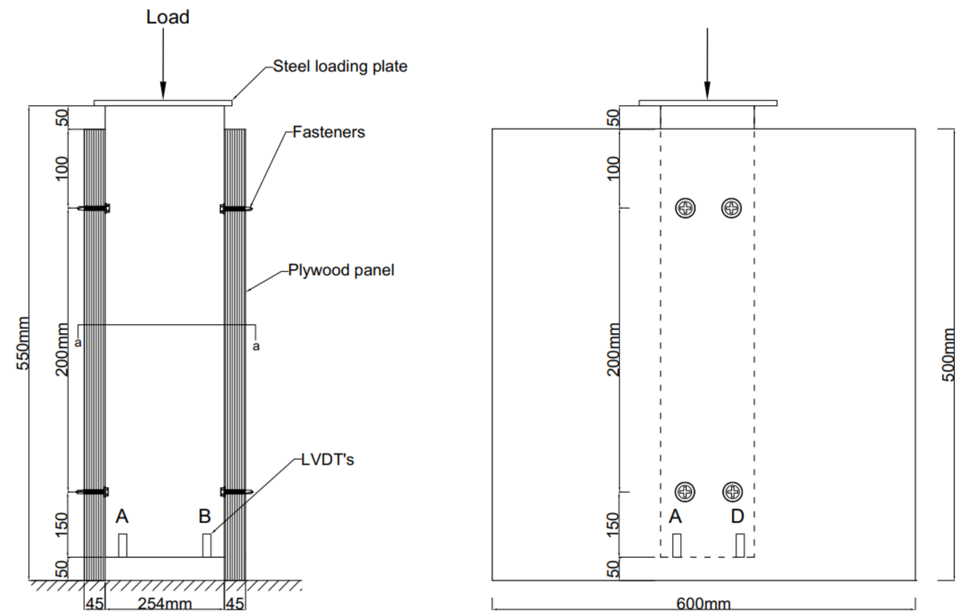

(a) Elevation view

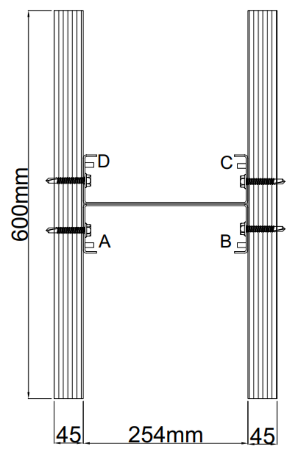

(b) Cross-section a-a view

Fig. 8 Push-out specimens schematic view

Table 4 Mechanical properties of the connectors

Type of connection	Diameter(mm)	Length(mm)	Grade	Yield strength (MPa)	Ultimate strength (MPa)
Self-drilling screw	6	50	-		425
Coach screw	12	55	4.6	240	400
Nut and bolt	12	60	4.6	240	400

(a) Self-drilling screw (b) Coach screw (c) Nut and bolt

Fig. 9 Three different types of fastener used in push-out tests

plywood panels was measured using four LVDTs (linear variable differential transformers) at the end of both beams. The LVDTs were fixed to the plywood panels, and four 60x60x6mm steel brackets were fixed to the CFS joist flange. The LVDTs were appropriately levelled and in contact with steel brackets to measure the relative slip due to the applied loading.

2.2.3 Load application

The specimens were loaded as per the procedure specified in BS EN 26891:1991(British Standard, 1991). The loading procedure in accordance with the standard is depicted in Fig. 11. A preliminary test was conducted from each series to determine the ultimate load, F_u. F_u is the load that corresponds to the failure of the specimen or a 15mm slip recorded during the test. Based on F_u (ultimate load) from the preliminary test, F_{est} (estimated failure load) was obtained for the rest of the test. F_{est} is essential for loading, unloading and reloading cycles as per the standard. Initially, the load was increased from 0 to $0.4F_{est}$ and was maintained at $0.4F_{est}$ for 30 s. After that, unloading of the specimen was done from $0.4F_{est}$ to $0.1F_{est}$, and the load was maintained for 30 s at $0.1F_{est}$. And finally, the load was increased up to $0.7F_{est}$ at a constant rate of load, and above $0.7F_{est}$, a constant rate of slip was used until the failure of the specimen. The displacement rate for the specimen with self-drilling screws was 1mm/min, while for the specimen with coach screws and nut and bolts was 2mm/min. All the specimens failed at about 11 to 15 minutes, which aligns with the total testing time specified in the BS EN 26891.

3. Discussion of Push-out Test Results

The distinct failure mode of the specimens and load-slip curves showing the average response from each test series are discussed and presented in this section. All specimens were in the elastic stage at the initial loading state; therefore, the slope had a linear relationship with the applied loading. With the increase of loading, friction between the CFS joist flange and the plywood became apparent, and the slow crushing sound of the plywood could be plainly heard. For the specimens with coach screw and nut and bolt, the failure criteria for the specimen was taken as 15mm slip as mentioned in BS EN 26891. It is worth mentioning that the specimens with coach screws and nut and bolts exhibited higher load capacity, but once the 15 to 18 mm joint slip was recorded, loading was stopped as the significant bearing of fasteners into the plywood panels had occurred prior to the peak load. However, for the specimens with self-drilling screws, the specimen failed at around 4 to 5 mm joint slip resulting in the shear failure of the screw itself. None of the tested specimens showed any splitting of the plywood from the CFS flange.

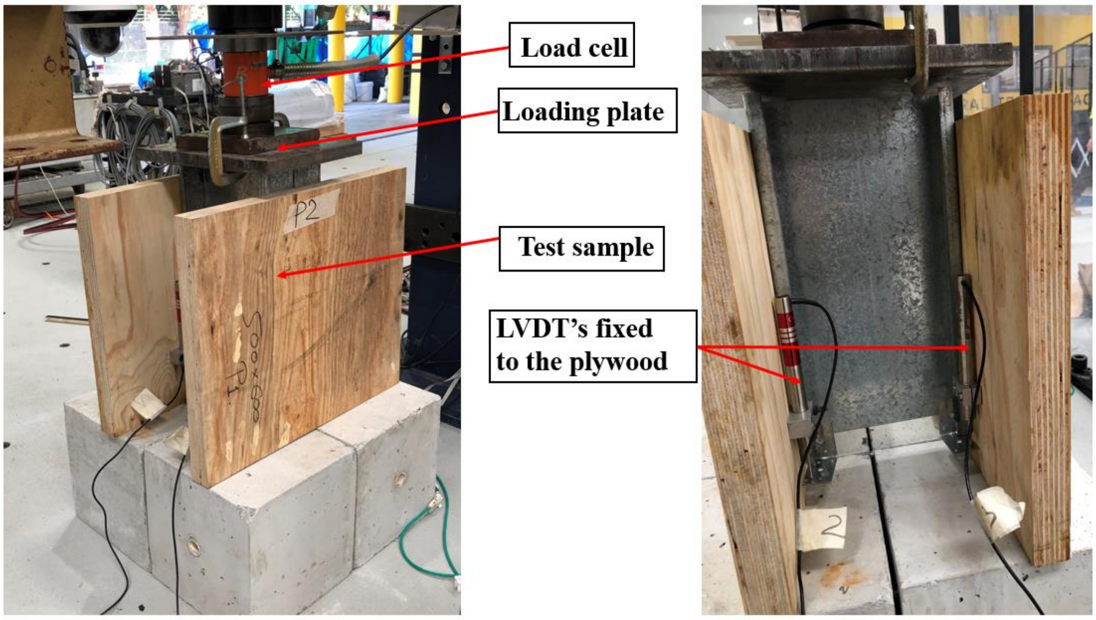

Fig. 10 Push-out test setup

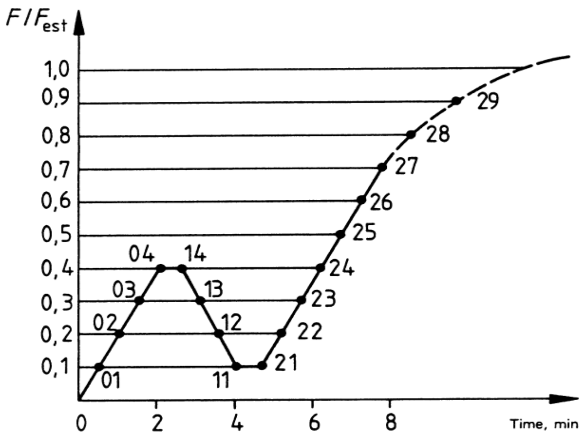

Fig. 11 Loading procedure adopted in push-out tests as per BS EN 26891:1991(British Standard, 1991)

(a) Shear failure under the head of the screw

(b) Bending failure

Fig. 12 Failure modes of the specimens with self-drilling screw

3.1 Modes of failure

3.1.1 Connections with self-drilling screws

All the specimens ultimately failed because of shear failure under the head of the screws. However, bending failure of the screws and their bearing into the plywood was also observed. The failure mode of the connection is shown in Fig. 12. Since the screw head was effectively restrained in the CFS joist flange, rotation of the screw was prevented. As loading increased, the screw was pressed against the flange and started to yield in bending. Further movement of CFS joists ultimately detaches the screw head from its body.

3.1.2 Connections with coach screws

The failure mode of the push-out specimens with coach screw connections is shown in Fig. 13. In these specimens, crushing of the plywood around the fastener was observed. The extent of the crush zone in plywood was almost double the size of the coach screw. Almost on every fastener, a plastic hinge occurred under the head of the coach screw. The formation of the plastic hinge can be attributed to the fact that when force was applied on the CFS joist, which gets transferred to the connection joints and with the increasing load coach screw yielded in flexure forming the plastic hinge and provide a ductile failure. The loading of the samples were stopped when 15mm to 17mm slip was recorded. It is noteworthy to mention that none of the samples showed any deformation of CFS joist or splitting of the plywood panels.

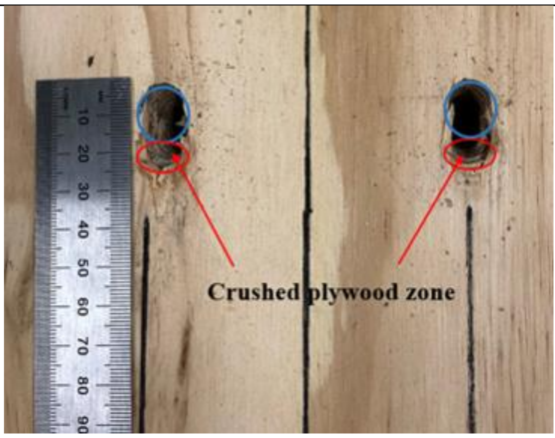

(a) Crushing of plywood

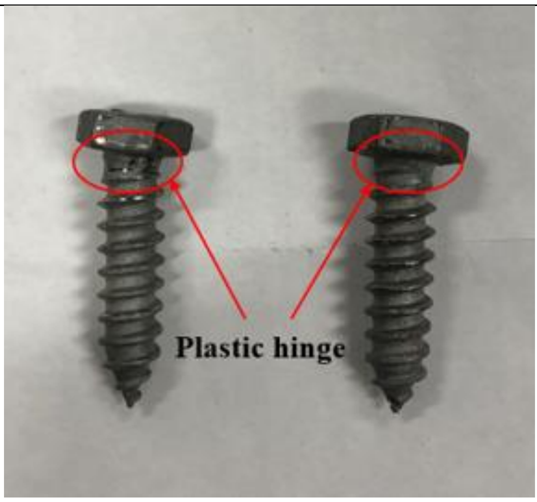

(b) Formation of plastic hinge

Fig. 13 Failure modes of the specimens with coach screws

3.1.3 Connections with nut and bolt

All the tested specimens were within the elastic stage during the initial stage of loading, and hence there was linear relationship between the slip and applied loading. With the increasing load plywood panel was squeezed by bolts and hence local damage of the timber as shown in Fig. 14(a) and 14(c) was observed. All the push-out specimens ultimately failed because of the bending of the fastener and its significant bearing pressure on the plywood that crushed it. When the specimen was loaded, the load was perpendicular to the longitudinal axis of the bolt. Because the head of the bolt was restrained to the plywood panel while the CFS joist effectively restrained the threaded part with nut, subtle plastic hinge formation is developed as shown in Fig. 14(b) at the near middle part of the bolt, which lies in the shear interface between the plywood panel and CFS joist as demonstrated in Fig. 15. As mentioned in the earlier section, slip up to 15mm was recorded, and the specimen loading was stopped. If the loading had continued beyond 15mm slip, a more distinctive plastic hinge could be seen on the bolt. Similar to the coach screw connection, the size of the crush zone in these connections is also double the size of the fastener. Fig.14 demonstrate the failure mode observed in these type of connections. No splitting of plywood panels or significant deformation of the CFS section was observed.

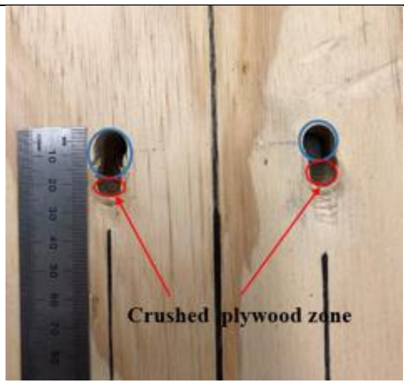

(a) Crushing of plywood

(b) Bending of bolt

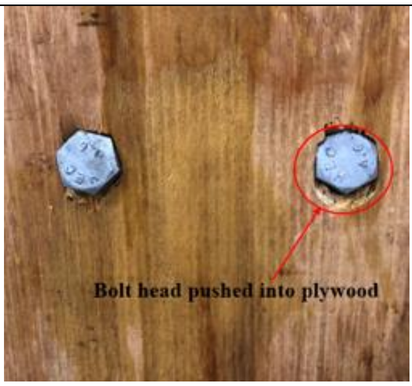

(c) Bearing of bolt head into plywood

Fig. 14 Failure modes of the specimens with nut and bolt

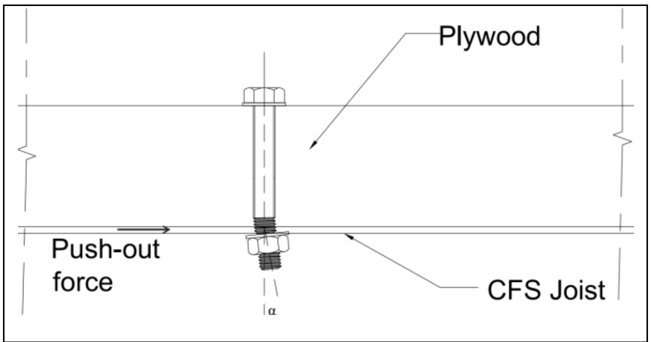

Fig. 15 Demonstration of bending developed on bolt

3.2 Load-slip behaviour of connections

When a composite cold-formed steel and timber beam assembly is loaded, the load is transferred from the structural sheathing through the connectors into the framing beneath the sheathing. It is well known that the amount of load that can be shared is dependant on the amount of slip that arises between two members or materials. This slip value, also known as slip modulus, helps to understand the extent of composite action in the assembly (Johnson and Molenstra, 1991; Couchman, 2016). This section discusses the load-slip responses of each connection type, and the slip modulus of each connection type is calculated. The calculated slip modulus value represents the stiffness of the shear connection. Higher the slip modulus value, the higher the ductility of the connection, which means an increase in the rigidity of the composite assembly and, therefore, the effective moment of inertia. When a composite assembly has a higher moment of inertia, it leads to increased strength capacities.

3.2.1 Connections with self-drilling screws

The load-slip response of the connections with size 14 (6mm diameter) self-drilling screws is shown in Fig.16. The load-carrying capacity P_u , and stiffness $K_{0.4}$ or slip modulus K_s of the connections are provided in Table 5. Normalised slip modulus, which is the slip modulus value per connector, is also calculated and tabulated in Table 5. The slip stiffness value $K_{0.4}$ or slip modulus is the value at 40% of the peak load F_{max} and is considered as the initial stiffness of the connections. The value of slip modulus is determined as per the steps outlined in BS EN 26891:1991. In Fig. 16, the average of tests curve is obtained by mathematical analysis of the three test curves in a graphical analysis tool called Origin pro (OriginPro-Graphing and Analysis tool, 2021). It was found that the initial stiffness or slip modulus was higher than the pre-peak stiffness (after 40% of the ultimate load) for this type of connections. The additional initial resistance for the screw connections was due to the self-drilling process which do not require pre-drilled hole and the existence of small pre-tension force. However, early slip were recorded for this type of connections because the head of the screw was in contact with the flange of CFS joist, and as the loading was applied through the joist the screw started to yield in bending under the head. A sudden drop in load, as can be seen on Fig.16, was found in all the specimens due to shear failure of the screw. From Table 5, it can be seen that load carrying capacity per self-drilling screw connector is 4.028 kN and the normalised slip modulus for the connector is 2.19 kN/mm.

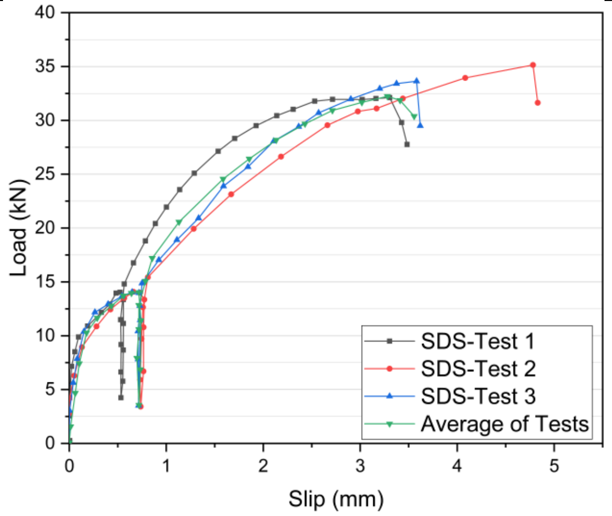

Fig. 16 Load slip response of specimens with self-drilling screws

Table 5 Load-carrying capacity and slip modulus of self-drilling screw shear connectors

Self-drilling screw (SDS)	Load at failure, P_u (kN)	Slip modulus, K_s (kN/mm)	Normalised slip modulus (kN/mm)
Test 1	32.2	22.1	2.76
Test 2	35.1	15.93	1.99
Test 3	33.6	17.63	2.2

3.2.2 Connections with coach screws

The load versus slip behaviour of the connections that utilise M12 coach screw (CS) connectors is shown in Fig. 17. Furthermore, the peak load-carrying capacity, slip modulus K_s (initial stiffness), and normalised slip modulus of the coach screw connections are provided in Table 6. As a joint slip of 15 mm is considered the failure of connections as per BS EN 26891, the peak load-carrying capacity is the load that coincides with the 15 mm slip. Hence, the average ultimate load at 15mm slip for the coach screw connections is 82.5 kN. The coach screw connections require pre-drilled holes in both CFS and plywood panels, hence the initial and pre-peak stiffness of this type of connections are similar as the material yielding of the composite assembly took place initially and gradually before damaging connector itself. From Fig. 17 and Table 6, it can be depicted that the load-carrying capacity per M12 coach screw connector is 10.35 kN and the normalised slip modulus for the connector is 1.36 kN/mm.

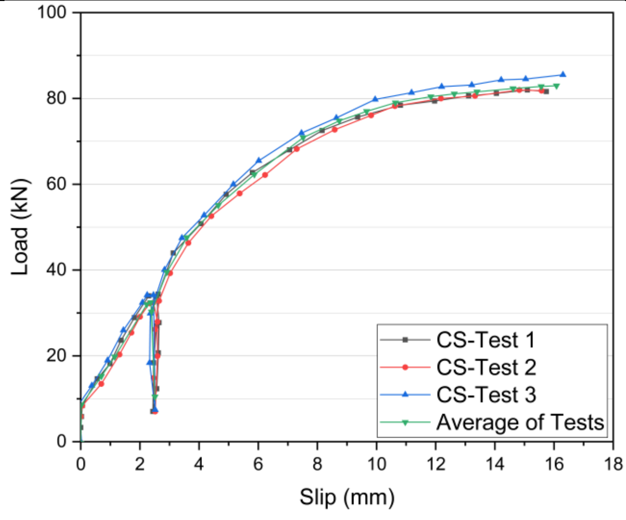

Fig. 17 Load slip response of specimens with coach screws

Table 6 Load-carrying capacity and slip modulus of coach screw shear connectors

Coach screw (CS)	Load at failure, P_u (kN)	Slip modulus, K_s (kN/mm)	Normalised slip modulus (kN/mm)
Test 1	81.98	11.39	1.42
Test 2	82	10.63	1.32
Test 3	84.5	11.38	1.42

3.2.3 Connections with nut and bolt

The load versus slip behaviour of the connections that utilise M12 nut and bolt (NB) connectors is shown in Fig. 18. In addition, the peak load-carrying capacity, slip modulus K_s (initial stiffness), and normalised slip modulus of the nut and bolt connections are provided in Table 7. The load-slip behaviour was consistent for all the tests, and this connection demonstrated high initial stiffness and strength than the other two. Up to 10 kN load, there was no slip between CFS and plywood panel, and after that, the response was almost linear till it reached 40% of the estimated load. The no-slip stage was due to the pre-tensioning of the bolts, which resulted in larger friction between the plywood panels and CFS joists interface. So with the increasing load, slip increased proportionally and was linear up to 40% of the ultimate load. M12 nut and bolt is a strong connector for the plywood and CFS assembly, and hence as a result material yielding started gradually first before any clear damage on the connector itself. The average ultimate load at 15mm slip for the nut and bolt connections is 132 kN. Nut and bolt connectors continued to increase in load capacity even after a slip of 15mm. The load-carrying capacity per M12 nut and bolt connector is 16.5 kN, and the normalised slip modulus for each connector is 2.75 kN/mm.

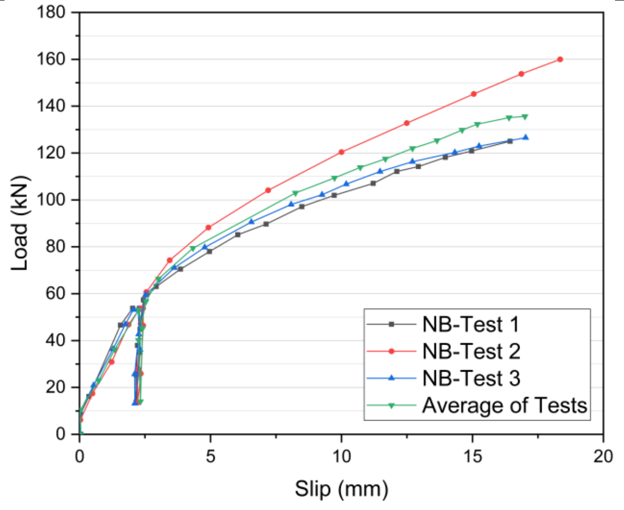

Fig. 18 Load slip response of specimens with nut and bolt

Table 7 Load-carrying capacity and slip modulus of nut and bolt shear connectors

Nut and bolt (NB)	Load at failure, P_u (kN)	Slip modulus, K_s (kN/mm)	Normalised slip modulus (kN/mm)
Test 1	121	22.91	2.86
Test 2	145	22.18	2.77
Test 3	123	21.85	2.73

3.3 Summary of test results

The summary of test results obtained from all the push-out specimens in terms of their mean values is presented in Table 8. Among the three different types of shear connectors tested, M10 nut and bolt (NB) connection exhibited better performance in terms of load-carrying capacity and stiffness. Self-drilling screw (SDS) connections demonstrated stiffer response when compared against all the coach screw (CS) connections. However, the important distinction here is SDS connections, despite being stiffer showed loss of stiffness with the increasing load; while CS connections demonstrated to retain stiffness with increasing load.

In accordance with BS EN 12512 (CEN, 2005), the ductility of the connection for each specimen is also calculated according to Equation (1)

$$D = \frac{V_u}{V_y} \quad (1)$$

Where V_u and V_y are the ultimate and yield slips, respectively. In these push-out tests, yield slip refers to the slip of connection joint corresponding to the yield load, and ultimate slip refers to the slip of connection joint corresponding to the yield load. The ultimate load slip for both CS and NB connectors is taken to be 15mm in line with BS EN 26891. Regarding connection ductility, the test result suggests that NB connectors offer more ductile connections followed by CS and SDS, respectively. A higher ductile connection value means the ability of the connection joint to undergo larger slip in the plastic range without reducing strength. Hence, from both serviceability and ultimate state point of view, nut and bolt shear connector demonstrated to be the best choice connection in the construction of composite cold-formed steel and timber flooring system. Similarly, in the serviceability state, self-drilling screws exhibited better stiffness than coach screws; however, coach screws proved to have enhanced performance than self-drilling screws in the ultimate state.

Table 8 Summary of key test results (mean values) for different shear connections

Type of shear connection	Load at failure, P_u (kN)	Slip modulus, K_s (kN/mm)	Ductility, D	Normalised slip modulus (kN/mm)
Self-drilling screw	32.23	17.59	4.8	2.19
Coach screw	82.8	10.89	5.3	1.36
Nut and bolt	132	21.96	7.1	2.75

4. Effective bending stiffness

The obtained sip modulus values are used to calculate the effective bending stiffness of a cold-formed steel and timber composite assembly. Steinberg et al. (2003) discussed the importance of calculating effective bending stiffness for designing timber-concrete composite floors, and a similar approach is used in this study. Shear bond coefficient, γ, should be calculated first to obtain the effective bending stiffness value of a composite assembly. Calculations are based on appendix B of Eurocode 5 (CEN, 2004).

$$\gamma = \frac{1}{1 + \frac{\pi^2 S E_t A_t}{K L^2}} \quad (2)$$

Where γ is a shear bond coefficient, S is the spacing of shear connectors in mm, E_t is the modulus of elasticity of timber sheathing (MPa), As is the area of timber sheathing (mm^2), K is slip modulus (N/mm), and L is the length of member (mm). The effective stiffness $(EI)_{eff}$ of the cold-formed steel and timber composite assembly can be found using Equation (3).

$$(EI)_{eff} = E_t I_t + \gamma E_t A_t a1^2 + E_j I_j + E_j A_j a2^2 \quad (3)$$

Where I_t is the moment of inertia of timber sheathing, a1 is the distance between the centroid of timber sheathing and centroid of composite assembly, E_j is the modulus of elasticity of CFS joist, I_j is the moment of inertia of CFS joist, A_j is the area of CFS joist, a2 is the distance between the centroid of CFS joist and composite assembly. The distance between the CFS joist centroid and centroid of composite assembly can be found from Equation (4).

$$a2 = \frac{\gamma E_t A_t (h_j + h_t)}{2(\gamma E_t A_t + E_j A_j)} \quad (4)$$

Fig. 18 shows the centroid location of composite assembly and value of a1 and a2 for a composite cold-formed steel and plywood beam. Based on the results of material tests and push-out tests as discussed in this paper, a simplified calculation is done to determine the effective bending stiffness of the composite assembly when three different shear connectors are used. The calculated effective bending stiffness is compared to the bending stiffness of the CFS joist alone. Tables 9 and 10 summarise the calculation of the shear bond coefficient and effective bending stiffness for each test series mean value.

Table 9 Calculation of shear bond coefficient

Type of shear connection	K_N (N/mm)	S (mm)	E_t (MPa)	A_t (mm^2)	I_t (mm^4)	E_j (MPa)	A_j (mm^2)	I_j (MPa)	γ
SDS	2190	200	9290	27000	4556250	207000	1093	10326810	0.099
CS	1360	200	9290	27000	4556250	207000	1093	10326810	0.0642
NB	2750	200	9290	27000	4556250	207000	1093	10326810	0.12

Table 10 Calculation of effective bending stiffness of the composite assembly

Type of shear connection	γ	E_jI_j ($N.mm^2$)	EI_{eff} ($N.mm^2$)	Stiffness increment (%)
SDS	0.099	2.13×10^{12}	2.68×10^{12}	25.5
CS	0.0642	2.13×10^{12}	2.52×10^{12}	18
NB	0.12	2.13×10^{12}	2.78×10^{12}	30.2

As can be seen from Table 10, the effective bending stiffness increased by 25.5%, 18% and 30.2% for SDS, CS, NB, respectively, over the stiffness of cold-formed steel joist alone. Hence, this proves that taking into account the shear bond coefficient γ, which is present as a result of the slip modulus of the shear connector, composite action is present in cold-formed steel and timber composite assembly.

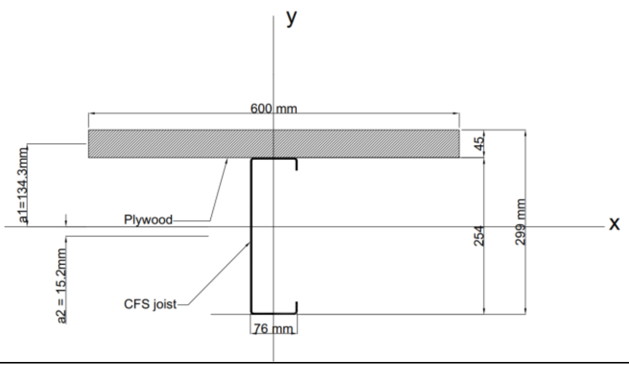

Fig. 19 Location of centroid in composite assembly of CFS joist and plywood sheathing

5. Conclusions

Nine push-out tests were conducted to study the load-slip response of three different types of shear connections supplemented by a series of material tests. Size 14 (6mm diameter) self-drilling screw (SDS), M12 coach screw (CS), and M12 nut and bolt (NB) connection joints were investigated in terms of slip modulus or initial stiffness and ductility. The load-carrying capacity and stiffness of the connections are of prime importance for evaluating the feasibility of any connectors. Furthermore, the combination of both values must be considered from an economical and efficient design point of view. A stiffer connection, for example, results in a higher effective bending stiffness of the composite cold-formed steel flooring system. Higher connection stiffness minimises deflection, which typically governs the design of a lightweight flooring system. In these push-out tests, self-drilling screws demonstrated stiffness higher than coach screw and lower than nut and bolt while coach screw, as expected, showed higher ductility than self-drilling screw and lower than nut and bolt. Nut and bolt shear connectors exhibited higher stiffness and ductility, showing it to be the best connection choice for constructing a composite cold-formed steel and timber flooring system. The increment of the effective bending stiffness by 25.5%, 18% and 30.2% for SDS, CS, NB composite assembly respectively, over the stiffness of cold-formed steel joist alone demonstrated the importance of mobilising composite action while designing composite cold-formed steel and timber flooring system. In current design of composite cold-formed steel and timber assemblies this composite action is not taken into consideration due to lack of research and understanding of the effective or composite bending stiffness in these assemblies. Taking into consideration, composite action might result in decreased member sizes or increased spacing of members, resulting in a more cost-effective design. Furthermore, improved understanding of effective stiffness can lead to more accurate vibration design in such lightweight flooring systems.

Further experimental push-out tests and finite element model development is ongoing to study the influence of various parameters on the load-slip behaviour of CFS and timber connections.

Acknowledgements

The authors would like to thank Peter Brown of the UTS tech lab for providing guidance throughout the testing.

References

British Standard 1991. BS EN 26891:1991 Timber structures-Joints made with mechanical fasteners.

Cen 2004. EN 1995-1-1:2004 Eurocode 5: Design of timber structures-Part 1-1: General-Common rules and rules for buildings. European Committee for Standardization.

Cen 2005. BS EN 12512 Timber structures-Test methods-Cyclic testing of joints made with mechanical fasteners. European Committee for Standardization.

Couchman, G. H. 2016. Minimum degree of shear connection rules for UK construction to Eurocode 4. Steel Construction Institute.

Far, H. 2019. Dynamic behaviour of unbraced steel frames resting on soft ground, *Steel Construction,* 12 (2), 135–140.

Far, H. 2020. Flexural Behavior of Cold-Formed Steel-Timber Composite Flooring Systems. *Journal of structural engineering,* 146**,** 06020003.

Hassanieh, A., Valipour, H. R. & Bradford, M. A. 2016. Load-slip behaviour of steel-cross laminated timber (CLT) composite connections. *Journal of Constructional Steel Research,* 122**,** 110-121.

Hassanieh, A., Valipour, H. R. & Bradford, M. A. 2017. Composite connections between CLT slab and steel beam: Experiments and empirical models. *Journal of Constructional Steel Research,* 138**,** 823-836.

Johnson, R. P. & Molenstra, N. 1991. Partial shear connection in composite beams for buildings. *Proceedings - Institution of Civil Engineers. Part 2. Research and theory,* 91**,** 679-704.

Karki, D. & Far, H. 2021. State of the art on composite cold-formed steel flooring systems. *Steel Construction.*

Karki, D., Far, H. & Saleh, A. 2021. Numerical Studies into Factors Affecting Structural Behaviour of Composite Cold-Formed Steel and Timber Flooring Systems. *Journal of Building Engineering***,** 102692.

Kyvelou, P., Gardner, L. & Nethercot, D. A. 2017. Testing and Analysis of Composite Cold-Formed Steel and Wood–Based Flooring Systems. *Journal of Structural Engineering,* 143.

Kyvelou, P., Gardner, L. & Nethercot, D. A. 2018. Finite element modelling of composite cold-formed steel flooring systems. *Engineering Structures,* 158**,** 28-42.

Lakkavalli, B. S. & Liu, Y. 2006. Experimental study of composite cold-formed steel C-section floor joists. *Journal of Constructional Steel Research,* 62**,** 995-1006.

Li, Y., Shen, H., Shan, W. & Han, T. 2012. Flexural behavior of lightweight bamboo–steel composite slabs. *Thin-Walled Structures,* 53**,** 83-90.

Loss, C. & Davison, B. 2017. Innovative composite steel-timber floors with prefabricated modular components. *Engineering Structures,* 132**,** 695-713.

Originpro-Graphing and Analysis Tool 2021. OriginPro, Version number 2021. OriginLab Corporation, Northampton, MA, USA.

Parnell, R., Davies, B. W. & Xu, L. 2010. Vibration Performance of Lightweight Cold-Formed Steel Floors. *Journal of structural engineering,* 136**,** 645-653.

Saleh, A., Far, H., Mok, L. 2018. Effects of different support conditions on experimental bending strength of thin walled cold formed steel storage upright frames. *Journal of Constructional Steel Research*, 150, 1–6.

Standard Australia 1996. AS1393:1996 Coach screws-Metric series with ISO hexagon heads. SAI Global.

Standard Australia 2000. AS1110.1-2000 ISO Metric hexagon bolts and screws. SAI Global.

Standard Australia 2002. AS3566.1-2002; Self-drilling screws for buidling and construction industries-Part 1. SAI Global.

Standard Australia 2007. AS 1391-2007 Metallic materials - Tensile testing at ambient temperature. Standard Australia: SAI Global.

Standard Australia 2012. AS/NZS 2269.1:2012 Plywood-Structural, Part 1: Determination of structural properties-Test methods. Australia: SAI Global.

Steinberg, E., Selle, R. & Faust, T. 2003. Connectors for Timber-Lightweight Concrete Composite Structures. *Journal of structural engineering,* 129**,** 1538-1545.

Tabatabaiefar, H..R., Mansoury, B., Khadivi Zand,M.J. & Potter, D. 2017. Mechanical Properties of Sandwich Panels Constructed from Polystyrene/Cement Mixed Cores and Thin Cement Sheet Facings. *Journal of Sandwich Structures and Materials*, 19 (4), 456-481.

Wang, L. & Young, B. 2014. Design of cold-formed steel channels with stiffened webs subjected to bending. *Thin-Walled Structures,* 85**,** 81-92.

Xu, L. & Tangorra, F. M. 2007. Experimental investigation of lightweight residential floors supported by cold-formed steel C-shape joists. *Journal of Constructional Steel Research,* 63**,** 422-435.

Zhou, X., Shi, Y., Xu, L., Yao, X. & Wang, W. 2019. A simplified method to evaluate the flexural capacity of lightweight cold-formed steel floor system with oriented strand board subfloor. *Thin-Walled Structures,* 134**,** 40-51.